

Wearable pressure sensing for lower limb amputees

Zhonghai Lu, Wenyao Zhu, Yizhi Chen Josephine Charnley

*KTH Royal Institute of Technology
Stockholm, Sweden*

Valter Dejke

*Lusstech
Sedgefield, UK*

RISE Research Institutes of Sweden

Mölndal, Sweden

Andrii Pomazanskyi

*Nuromedia GmbH
Cologne, Germany*

Siu-Teing Ko Begum Zeybek, Pouyan Mehryar, Zulfiqur Ali Michalis Karamousadakis

*Össur
Reykjavík, Iceland*

*Teesside University
Middlesbrough, UK*

*TWI Hellas
Halandri, Greece*

Dejiu Chen
*KTH, ITM School
Stockholm, Sweden*

Abstract—Pressure sensing in prosthetic sockets is valuable as it provides quantified data to assist prosthetists in designing comfortable sockets for amputees. We present a wearable pressure sensing system for lower limb amputees. The full system consists of three essential elements from sensing scheme (wearable sensors, sensor calibration and deployment), electronic measurement system (embedded hardware and software), to time-series database and visualization. The full system has been successfully applied in clinical trials to effectively collect pressure data in real-time.

Index Terms—Wearable sensors, prosthetic socket, lower limb amputees, prosthesis, electronic measurement system, ESP32

I. INTRODUCTION

Limb amputations cause serious physical disabilities that compromise the quality of life of amputees. There are 40 million amputees in the world and approximately 215,000 amputation surgeries performed each year (around 90% are lower limb amputees) [1]. This number is expected to increase, due to an aging population and a corresponding higher incidence of diabetes and vascular diseases [2]. The demand for efficient prosthetic socket design grows steadily due to an increasing number of amputees and lack of efficiency in designing comfortable sockets.

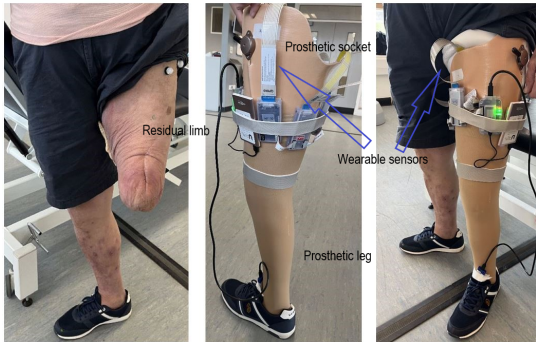


Fig. 1. Wearable sensors embedded in socket for transfemoral amputee

In response to this grand challenge, a current trend is to enable a quantitative data-analytic approach to assist prosthetists to evaluate patient comfort, socket fit and shape, and rectify prosthetic sockets for amputees [3], [4]. With such an approach, wearable pressure sensors are placed into a socket. One example is shown in Figure 1, and an electronic measurement system acquires the measurement data from the sensors. The collected pressure data can then be analyzed to

generate relevant information to help prosthetists to monitor, evaluate the performance of the socket and adjust the socket design for comfort and comfort enhancement.

The paper presents a pressure-measuring system for efficient sensing, data acquisition and exploration for lower-limb amputees. The entire system includes a sensing subsystem, an embedded microprocessor-based subsystem, and a storage and visualization subsystem. Specifically, we differentiate our system from existing measurement systems as follows.

- We use printed sensors with QTSS™ materials, and strip-based sensor organization. The sensors are calibrated using a proportional-shift method enabling on-site calibration of approximately three sensors per minute.
- We adopt a dual-core ESP32 System-on-Chip (SoC), which allows data acquisition and transmission for storage in a seamless producer-consumer processing pipeline.
- The full system has been successfully applied in real-life clinical trials for pressure data collection after development and validation in performance and correctness.

In the remainder, we first discuss related work in Section II and then describe our system in detail with focus on design principles and considerations in Section III. Section IV presents the application of the system in clinical trials. Finally, we conclude in Section V.

II. RELATED WORK

Intra-socket pressure measurement has long been interesting to facilitate socket design and fit. As reported in [5], different types of sensors such as strain gauges, piezo-resistive, capacitive, and optical sensors etc. have been used for pressure measurements. Recently, inserting flexible sensors directly into the socket has become popular. Several commercial solutions have been developed such as the piezo-resistive sensors from Tekscan, Inc. USA and the capacitive sensors from Novel GMBH, Germany. A pressure sensor system has been developed [6] using 3D-printed capacitive stress sensor [7]. Also, printed sensors using conductive inks [8] and textile-based pressure sensors [9], [10] are introduced to the socket stress measurement. In our system, we use QTSS™ quantum conduction printed sensors [11].

In lower limb prostheses, measurements and mapping interface pressure to amputees' anatomy are commonly performed using commercially available pressure monitoring systems [12]–[16]. In the study of interfacial pressure of patients during

ascent and descent on stairs, Ali *et al.* [15] have used four Tekscan F-Socket® transducers [17] with 96 sensors on each strip to cover the stump. Similar pressure measurements have been conducted using three quadratic pressure sensor arrays (Novel Pliance® S2052 [18]) of 16 cm^2 with 4×4 sensors integrated [16].

Despite the commercial pressure sensing systems being available, their technical design details and, in particular, the design considerations of these measurement systems have seldomly been disclosed in literature. Thus it can be difficult to reason about their design choices.

III. THE PRESSURE SENSING SYSTEM

A. Overview

Figure 2 depicts an overview of the pressure-sensing system, which consists of three subsystems as follows.

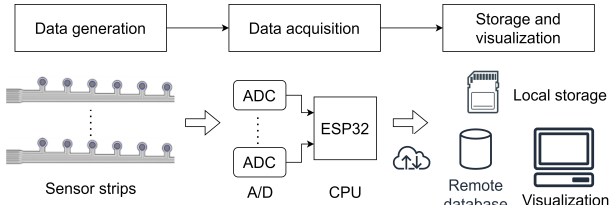


Fig. 2. The pressure-sensing system

- 1) Sensor subsystem: Conformable printed pressure sensors using QTSS™ materials were developed as sensor strips, each strip hosting multiple sensors. This allows us to flexibly deploy sensor strips in desired locations and reduce redundancy [19] inside socket to capture interesting points of measurement across the inner socket.
- 2) Electronic measurement subsystem: The purpose of measurement is to acquire the generated data from the sensors. It mainly consists of an Analog/Digital Conversion (ADC) interface and an embedded ESP32-based hardware and software.
- 3) Storage and visualization subsystem: The acquired data can be stored locally in an SD card and transmitted via the Internet to a remote server. The collected data are stored as time-series data in a database for visualization.

B. Sensor subsystem

1) *QTSS™ sensor and sensor strip:* In our pressure-sensing system, we use QTSS™ sensors [11], which are flexible wearable sensors. The materials are magnetite-based, anisotropic and change from ‘insulator’ to ‘conductor’ under pressure, becoming increasingly conductive in response to the amount of applied force. Thus a QTSS™ sensor works as a variable resistor whose resistance R changes with the applied pressure, P , i.e., $R = f(P)$ (R is a function f of P). Using this property, we can conveniently measure the voltage V on the variable resistor in our electronic measurement system, thus obtaining V as a function g of pressure P , i.e., $V = g(P)$.

In practical use, we first characterize the function g for each sensor. Then, given a measured voltage V in an actual clinical trial, we can derive its corresponding pressure P by the inverse function $P = g^{-1}(V)$.

We adopt the strip-based sensor organization. Compared to an array-based sensor organization, it gives more flexibility to place the sensor strips with different density in a socket. Figure 3 shows a sensor strip with eight QTSS™ sensors printed on a PET (polyethylene terephthalate) substrate [11].

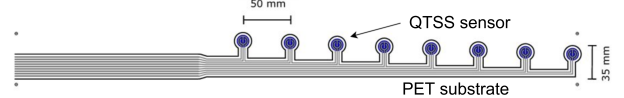


Fig. 3. Sensor strip

2) *Sensor calibration:* One challenge with printed sensors is that their pressure-response characteristic can drift. Calibration is thus needed for each sensor. In our approach, we use an *off-site major calibration* in the test room, combined with *on-site minor calibration* using a hand-held pressing device after the sensors are mounted in the socket. The major calibration is to obtain the sensor pressure characteristic curve g , and the on-site minor calibration is to tune g using proportional shift according to the sensor’s present property.

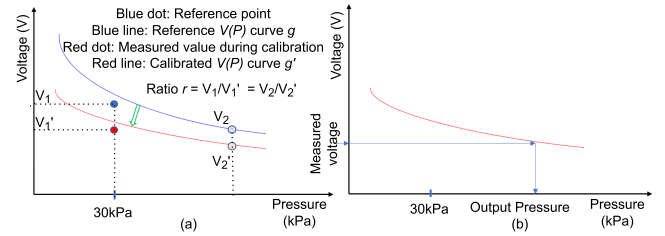


Fig. 4. Principle of sensor calibration

Figure 4(a) shows the principle of sensor calibration. The sensor pressure characteristic function g was obtained through the major calibration, which is used as the reference curve. Because of differences in the measuring conditions, the measurement point generated by the hand-held pressing device is typically deviated slightly from the position of the major calibration curve. During the on-site minor calibration, the hand-held pressing device was used to apply the known pressure of 30 kPa on a sensor to get the ‘present’ voltage (V'_1 vs. V_1) under this pressure. Thus we obtain a shifting ratio $r = V'_1/V_1$. The entire curve of g is then proportionally shifted towards the new measurement point, indicated by the red curve g' . The shifting ratio for all points on the curve is equal to $r = V'_1/V_1$. As shown in Figure 4(b), the calibrated curve g' is used to derive the pressure given a measured voltage.

C. Electronic measurement subsystem

1) *Overview:* Figure 5 gives a schematic view of the electronic measurement system, which consists of two main parts: ADC interface and ESP-32 microprocessor.

The pressure sensor functions as a variable resistor whose value changes in response to the force exerted on it. Due to its serial connection to another resistor with a constant value, the circuit works as a voltage divider. When force/pressure is applied on the sensor varies, the voltage divider generates varying analog voltage, which is then converted into digital levels through an ADC channel. Afterwards, the digitalized level signals are sampled from the SPI (Serial Peripheral Interface) bus by ESP32 under clock synchronization.

2) Design considerations for ADC: The ADC is a key component that determines how fast and how accurate we can sample data from the sensors. It shall be fast enough so that we can collect enough samples for data analysis. It shall be accurate enough so that we can get data with sufficient precision. Additionally, we need to consider its safe operation under unexpected circumstances, such as over voltage supply, and interfacing option with the microprocessor.

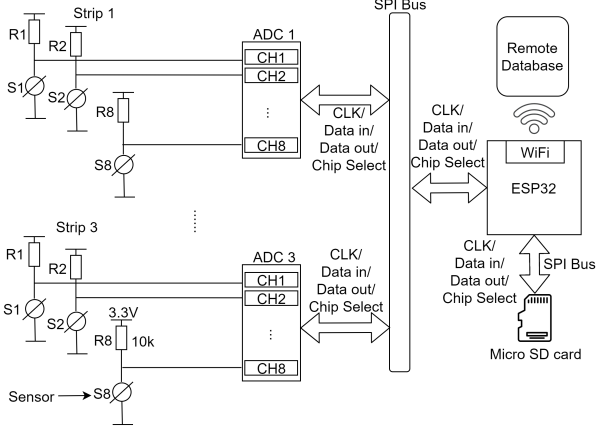


Fig. 5. ESP32 system reads data via SPI bus from the ADC channels

With the above considerations, instead of using built-in ADC in an embedded SoC, we have chosen to use an external ADC module, MCP3208, which is an 8-channel 12-bit ADC module. It has a maximum sampling rate of 100 kHz, removing the concern on the possible speed bottleneck from ADC modules. The 12-bit resolution gives a digital value range from 0 to 4095, which is of sufficiently high resolution to reflect meaningful pressure variation. The ADC module also satisfies the need for SPI interfacing, flexibility in voltage division, and safety (Over-voltage protection for each channel) etc.

3) Design considerations for the embedded platform: The choices for building such a microprocessor-based embedded system are many, due to a variety of options, such as Arduino, Raspberry Pi series etc. After considering all possibilities in performance, cost, and size, we have chosen to use ESP-32, ESP-WROOM32E, from Espressif Systems, which is a highly integrated SoC with Xtensa dual-core 240 MHz 32-bit microprocessor. Besides other necessary interfaces and parallel I/Os, we find that the dual-core structure fits very well for our data readout and data transmission purposes. In fact, we use one core to handle data readout from the ADC channels, and the other core to handle data storing and data transmission via Internet to a remote server for real-time streaming.

The communication interface between the ESP32 SoC and the peripheral devices is the SPI bus, which allows an easy extension of including more sensor strips and other sensors or peripherals in the system (limited by the number of I/O pins of the ESP32 SoC, though). The system also provides a connector for SD card used as a local storage space and Wi-Fi connection to Internet for remote storage in a database on the server. To isolate interference from other peripherals, writing/reading the SD card uses an independent SPI bus.

4) Design considerations for the embedded software: Rather than bare-metal program, the data processing software runs on top of the freeRTOS [20]. It can be divided into three tasks: data acquisition, data buffer management, data communication. Since the ESP32 SoC contains two identical CPU cores, this allows us to achieve a reasonable balanced task partitioning by loading tasks on both cores in a pipeline.

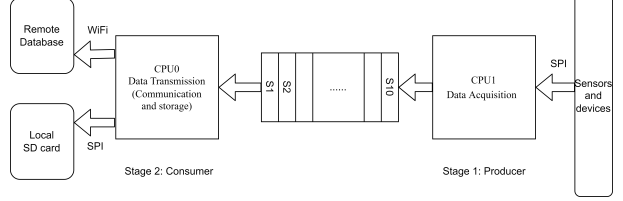


Fig. 6. Dual-core parallel processing under the producer-consumer paradigm

As shown in Figure 6, we employ a producer-consumer inter-process communication paradigm [21] to construct the data processing software. The data acquisition task running on CPU1 is the producer while the data transmission task running on CPU0 is the consumer. The producer communicates with the consumer via the shared data queue, which is supported by freeRTOS with xQueue functions.

- **Data production (acquisition):** On the producer side, CPU1 feeds the data queue with one sample a time as soon as it finishes the sample collection procedure.
- **Queue size and management:** The data queue is assigned in the physical memory by the data acquisition task. The queue size is N times of the data structure for one sample. The size N is configurable, and the default value is 10. The queuing policy is First-In First-Out (FIFO). Writing to the queue is blocking write (to avoid data over-written) and reading from the queue is non-blocking.
- **Data consumption (communication and storage):** On the consumer side, CPU0 checks the data queue periodically, and reads out the data into a local data buffer. By default, every 10 samples are encapsulated into one packet, which is then sent to the remote InfluxDB database via a reliable HTTP post and also written into the SD card.

In our current software loop, sampling one round of data (one frame or packet) from all sensing peripherals may take 50 ms, 20 ms, 10 ms (The OS task granularity is 10 ms) by configuration. Thus the data frame sampling rate can be 20 Hz, 50 Hz and 100 Hz, respectively.

D. Data storage and visualization subsystem

The data communication and storage task transmits sampled data to the InfluxDB database on the remote server and to the SD card as local backup. This redundant scheme allows the measurement data to be accessible through the database in real time and from the SD card after data collection. This ensures that even under network communication disturbances from Wi-Fi or Internet, the SD card can serve as a safe backup.

A graphical user interface (GUI) has been developed to visualize the time-series data with user interaction. The GUI allows the user to visualize the data in various forms, e.g., per sensor strip, per sensor or per exercise, for each amputee.

IV. CLINICAL TRIALS

The pressure-measuring system has been successfully developed and validated. Afterwards, it has been applied in multiple clinical trials in hospitals in UK and Spain. All trials were done with amputees after the trial protocols had been reviewed and approved by responsible national authorities^{1 2}.

A. Trial procedure

The procedure for applying the pressure-measuring system was well defined in a protocol before the actual conduct of the trials with amputees. This includes *pre-trial preparation*, *in-situ data collection*, *post-trial visualization*.

1) *Pre-trial preparation*: The pre-trial preparation includes mainly sensor-strip deployment and sensor calibration.

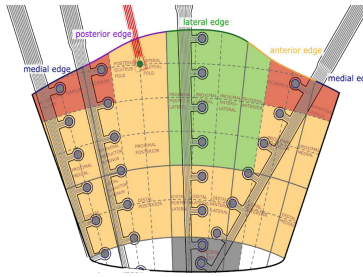


Fig. 7. Sensor-strip deployment



Fig. 8. Sensor strips in socket

Sensor-strip deployment: Figure 7 shows one example of the sensor-strip placement plan. The 2D map shows an unfolded inner surface. The colors show regions of high or low pressures and sensor strips are placed to cover pressure sensitive regions. More details are described in [22], [23]. According to the deployment scheme, the actual sensor strips are embedded into a socket, as shown in Figure 8.

Sensor calibration: After the sensor-strip deployment, the sensors were calibrated inside the socket. The simple proportional-shift method based on single-point sampling using the hand-held device allows us to quickly calibrate all sensor strips (5 strips, 30 sensors inside socket) in about ten minutes. Calibrations were conducted pre and post trial.

2) *In-situ data collection*: The trial tasks include Donning the socket with the system calibrated and installed, Static standing, Level ground walking, Stand to sit, Static sitting, Sit to stand, Ramp ascent, Ramp descent, Stair ascent, Stair descent, Doffing of the socket. During the trial tasks, the measured voltage data are continuously collected to the SD card. Besides the pressure data, a gait monitor was added to the sensing SPI bus to synchronously collect the gait information.

3) *Post-trial data visualization*: After each trial with an amputee, the collected time-series voltage data are stored into the time-series database on a remote server. The voltage data are converted into the pressure data using the inverse function of the calibrated $V(P)$ curve.

¹UK: Health Research Authority (HRA) and Medicines and Healthcare products Regulatory Agency (MHRA) approvals were obtained for (IRAS Project ID: 292614).

²Spain: Comité de Ética de la Investigación con medicamentos (CEIm) and Agencia Española de Medicamentos y Productos Sanitarios (AEMPS) approvals were obtained.

B. Trial results visualization

In all the trials, our system was able to acquire all measurement data correctly and without data loss. Each trial lasted up to 3 hours, generating about 65 MB data.

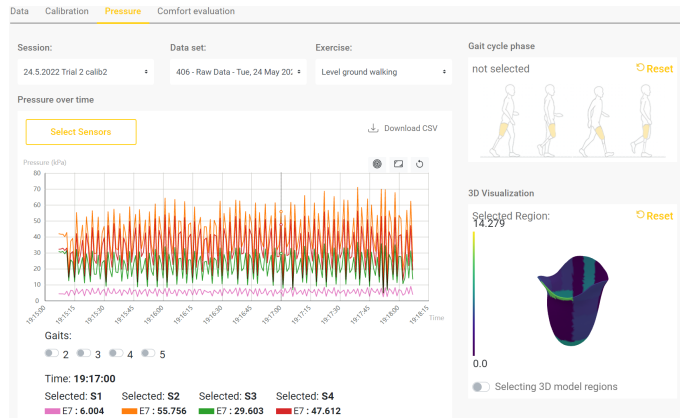


Fig. 9. The GUI and recorded time-series data for four sensors

Figure 9 shows the GUI and a screenshot showing time series data for four sensors on the sensor strips, S1E7, S2E7, S3E7, and S4E7 (Notation SxEy refers to sensor y on strip x). These are located on the proximal end of the lateral edge, anterior edge, medial edge, and posterior edge respectively. The pressure plot shows the cyclic pressure changes during level-ground walking (5 minutes from 7:15 to 7:20 pm). Note that S1E7 is on the proximal end of the lateral edge. It has readings, but not so visible in the plot due to its relatively small pressure magnitude. The GUI has implemented several practical functions to visualize the data. The pressure of the selected sensors from the dedicated strips will be imposed on a 3D model of a socket with a color coding of the pressure regions. Navigating through the GUI allows the user to filter the data by the exercises performed, applying various calibration values, check gait information, and download a .csv file for further analysis in external software.

V. CONCLUSION

We have presented a full conformable printed pressure-sensing system for measuring pressure distribution in the socket of lower-limb amputees, focusing on design principles and considerations. The system was customized for the specific needs of pressure measurement inside the prosthetic socket. The full system was validated and used in clinical trials to successfully collect data conveniently and without loss.

Our future work is to analyze the collected data from clinical trials so as to establish the relationship between the pressure distribution and the comfort level of socket. As such, the present empirical approach for socket design can be enhanced with quantitative data analytic methods.

ACKNOWLEDGMENT

This research was completed as part of the SocketSense project that has received funding from the European Union's Horizon 2020 research and innovation programme under grant agreement No 825429.

REFERENCES

- [1] Z. Ali and J. Gao, "Advanced sensor-based design and development of wearable prosthetic socket for amputees," <https://research.tees.ac.uk/en/projects/advanced-sensor-based-design-and-development-of-wearable-prosthet> [Accessed: May, 2022].
- [2] N. Sattar, A. Rawshani, S. Franzén, A. Rawshani, A.-M. Svensson, A. Rosengren, D. K. McGuire, B. Eliasson, and S. Gudbjörnsdóttir, "Age at diagnosis of type 2 diabetes mellitus and associations with cardiovascular and mortality risks: findings from the swedish national diabetes registry," *Circulation*, vol. 139, no. 19, pp. 2228–2237, 2019.
- [3] S.-T. Ko, F. Asplund, and B. Zeybek, "A scoping review of pressure measurements in prosthetic sockets of transfemoral amputees during ambulation: Key considerations for sensor design," *Sensors*, vol. 21, no. 15, 2021. [Online]. Available: <https://www.mdpi.com/1424-8220/21/15/5016>
- [4] M. Karamousadakis, A. Porichis, S. Ottikkutti, D. Chen, and P. Vartholomeos, "A sensor-based decision support system for transfemoral socket rectification," *Sensors*, vol. 21, no. 11, 2021. [Online]. Available: <https://www.mdpi.com/1424-8220/21/11/3743>
- [5] L. Paternò, M. Ibrahimi, E. Gruppioni, A. Menciassi, and L. Ricotti, "Sockets for limb prostheses: a review of existing technologies and open challenges," *IEEE Transactions on Biomedical Engineering*, vol. 65, no. 9, pp. 1996–2010, 2018.
- [6] P. Laszczak, M. McGrath, J. Tang, J. Gao, L. Jiang, D. Bader, D. Moser, and S. Zahedi, "A pressure and shear sensor system for stress measurement at lower limb residuum/socket interface," *Medical engineering & physics*, vol. 38, no. 7, pp. 695–700, 2016.
- [7] P. Laszczak, L. Jiang, D. L. Bader, D. Moser, and S. Zahedi, "Development and validation of a 3d-printed interfacial stress sensor for prosthetic applications," *Medical engineering & physics*, vol. 37, no. 1, pp. 132–137, 2015.
- [8] J. R. Camargo, L. O. Orzari, D. A. G. Araújo, P. R. de Oliveira, C. Kalinke, D. P. Rocha, A. Luiz dos Santos, R. M. Takeuchi, R. A. A. Munoz, J. A. Bonacini, and B. C. Janegitz, "Development of conductive inks for electrochemical sensors and biosensors," *Microchemical Journal*, vol. 164, p. 105998, 2021.
- [9] J. F. Saenz-Cogollo, M. Pau, B. Fraboni, and A. Bonfiglio, "Pressure mapping mat for tele-home care applications," *Sensors*, vol. 16, no. 3, p. 365, 2016.
- [10] J. Tabor, T. Agcayazi, A. Fleming, B. Thompson, A. Kapoor, M. Liu, M. Y. Lee, H. Huang, A. Bozkurt, and T. K. Ghosh, "Textile-based pressure sensors for monitoring prosthetic-socket interfaces," *IEEE Sensors Journal*, vol. 21, no. 7, pp. 9413–9422, 2021.
- [11] V. Dejke, M. Eng, K. Brinkfeldt, J. Charnley, D. Lussey, and C. Lussey, "Development of prototype low-cost QTSS™ wearable flexible more enviro-friendly pressure, shear, and friction sensors for dynamic prosthetic fit monitoring," *MDPI Sensors*, vol. 21: 3764, no. 11, 2021.
- [12] A. Polliack, R. Sieh, D. Craig, S. Landsberger, D. McNeil, and E. Ayyappa, "Scientific validation of two commercial pressure sensor systems for prosthetic socket fit," *Prosthetics and orthotics international*, vol. 24, no. 1, pp. 63–73, 2000.
- [13] A. Eshraghi, N. A. A. Osman, H. Gholizadeh, S. Ali, S. K. Sævarsson, and W. A. B. W. Abas, "An experimental study of the interface pressure profile during level walking of a new suspension system for lower limb amputees," *Clinical Biomechanics*, vol. 28, no. 1, pp. 55–60, 2013.
- [14] J. T. Kahle and M. J. Highsmith, "Transfemoral sockets with vacuum-assisted suspension comparison of hip kinematics, socket position, contact pressure, and preference: ischial containment versus brimless," *J Rehabil Res Dev*, vol. 50, no. 9, pp. 1241–1252, 2013.
- [15] S. Ali, N. A. A. Osman, A. Eshraghi, H. Gholizadeh, W. A. B. B. W. Abas *et al.*, "Interface pressure in transtibial socket during ascent and descent on stairs and its effect on patient satisfaction," *Clinical Biomechanics*, vol. 28, no. 9-10, pp. 994–999, 2013.
- [16] S. I. Wolf, M. Alimusaj, L. Fradet, J. Siegel, and F. Braatz, "Pressure characteristics at the stump/socket interface in transtibial amputees using an adaptive prosthetic foot," *Clinical Biomechanics*, vol. 24, no. 10, pp. 860–865, 2009.
- [17] Tekscan, Inc., "Tekscan medical sensor 9811E," <https://www.tekscan.com/products-solutions/medical-sensors/9811e> [Accessed: Dec, 2021].
- [18] Novel Electronics, "Pliance: Pressure and load distribution on hard or soft surfaces," <https://www.novel.de/products/pliance/> [Accessed: Mar, 2022].
- [19] W. Zhu, Y. Chen, S.-T. Ko, and Z. Lu, "Redundancy reduction for sensor deployment in prosthetic socket: A case study," *MDPI Sensors*, vol. 22, no. 9: 3103, April 2022.
- [20] freeRTOS.org, "Tensilica xtensa customizable processors freeRTOS demo," <https://www.freertos.org/index.html> [Accessed: Dec, 2020].
- [21] K. Jeffay, "The real-time producer/consumer paradigm: A paradigm for the construction of efficient, predictable real-time systems," in *Proceedings of the 1993 ACM/SIGAPP symposium on Applied computing: states of the art and practice*, 1993, pp. 796–804.
- [22] V. S. P. Lee, S. E. Solomonidis, and W. D. Spence, "Stump-socket interface pressure as an aid to socket design in prostheses for transfemoral amputees—a preliminary study," *Proceedings of the Institution of Mechanical Engineers, Part H: Journal of Engineering in Medicine*, vol. 211, no. 2, pp. 167–180, 1997.
- [23] E. S. Neumann, J. S. Wong, and R. L. Drollinger, "Concepts of pressure in an ischial containment socket: Measurement," *JPO: Journal of Prosthetics and Orthotics*, vol. 17, no. 1, pp. 2–11, 2005.